

Abstract

The ferrite grain size of a 22MnVNb6 microalloyed steel can be estimated by developing a relationship between ferrite grain size, austenitising temperature and cooling rate from austenitising time, temperature. An extended Hall-Petch relationship was used to estimate the yield stress from the estimation ferrite grain size. Heat treatment as the annealing was used to improve the tensile and hardness properties of the steel. It was shown that the best combination of tensile and hardness properties were achieved when a higher austenitising temperature was used. Transmission electron and optical microscopy were used to study the morphology of ferrite and pearlite formed by the heat treatments. The microstructural studies showed that partition of grain by as-cast state was probably the reason for austenite and ferrite grain size improvement. Considering the experimental results, maximum errors of 14.5% and 7.5% were found in the estimation of ferrite grain size and tensile strength, respectively.

Keywords

grain size, mechanical properties, Microalloyed Steel, Hall-Petch relationship

1 Introduction

The name “Microalloyed Steels” was first applied to a class of higher strength low carbon containing small additions of niobium and/ or vanadium. Any attempt at a rational definition of microalloying based on the increases in strength produced by small additions would now include aluminium, vanadium, titanium and of course niobium-treated steels. The effects of the microalloying elements are also strongly influenced by thermal treatments [1, 2]. The transformation product grain size control is an important parameter in thermal and mechanical processing of microalloyed steels. It has been well recognized that the tensile and hardness properties of steels are strongly related to the microstructure, specially the grain size [3, 4]. In the heat treatment of microalloyed low carbon cast steels involving the austenitising and cooling treatments, the parameters such as cooling rate and austenitising temperature and time have considerable influence on the ferrite grain size and tensile and hardness properties of the steels. It has been shown that accelerated cooling treatment refines the ferrite grain size while increasing the austenitising time and temperature increases the ferrite grain size. Several studies on accelerated cooling have been carried out, considering the relation of processing parameters and tensile and hardness properties to the microstructures [5]. In those studies the relationships presented for estimating ferrite grain size were deduced experimentally to relate the ferrite grain size to the cooling rate and prior austenite grain size [6-9]. The grain size estimation model presented by Umamoto et al., is extended in this research to develop a relationship between ferrite grain size, cooling rate, austenitising time, and temperature. The following Hall-Petch relationship is utilized to relate the yield stress to the ferrite grain size [10-14]

$$\sigma_y = \sigma_0 + Kd_\alpha^{-0.5} \quad (1)$$

where σ_y is the yield stress, σ_0 and K are constants, d_α the ferrite grain size. The grain size of a microalloyed steel has an important effect on its properties. This phenomenon is known in the literature as the grain size effect. As far as the tensile and hardness properties of the steel is concerned (such as yield and flow stress, ductility, hardness and fatigue limit), a refinement

¹ Department of Mechanical Engineering, Faculty of Engineering, Srinakharinwirot University, Ongkharak, Nakhon-nayok, 26120, Thailand

* Corresponding author, e-mail: pganwarich@yahoo.com

of the grain size generally results in an improvement of these properties at low temperature. Since the grain boundaries are known to block the movement of crystal dislocations, the grain size effect has been explained in term of the distance a dislocation can slip. The improved yield strength can be attained only by carefully controlled heat treatment. Normalizing and/or solution annealing come under consideration. Yield strength of microalloyed metallic material obeys extended Hall-Petch relationship [15, 16] as follows

$$R_y = R_o + \Delta R_a + \Delta R_g + \Delta R_p + \Delta R_t \quad (2)$$

Where R_o is friction stress, ΔR_a is related to solid solution strengthening being linearly proportional to the concentration of alloying elements, ΔR_g is a grain size contribution, ΔR_p is precipitation strengthening and is the proportional to precipitation potential, ΔR_t is matrix phase transformation strength.

1.1 Determination of austenite grain size distribution

Austenite grain size distribution can be recorded by photographing the microscopic picture and the determination requires measurement of each individual grain. Austenite grain size distribution in one dimension is the distribution of the lengths of linear intercepts through the grains. Metallographic techniques for measuring austenite grain size were originally base on point counting or linear intersection lengths (chords) distributions, the derivation by Spektor appears to be the first [17, 18]. The working formula is obtained [12] as below

$$N_v(j) = \frac{4}{\pi \Delta^2} \left[\frac{n_L(j)}{2j-1} - \frac{n_L(j+1)}{2j+1} \right] \quad (3)$$

Where $N_v(j)$ is the number of particles of mean diameter per unit volume in the interval $2j-1$, $n_L(j+1)$ is the number of chords per unit length of test line. The austenite grain size microstructures of entire the relevant samples representative photomicrographs were taken. In order to determine the austenite grain size, the samples were specially etched in a saturated picric acid solution at about 80°C [19, 20]. The austenite grain size was then measured at magnification 25× using a filler eyepiece. The degree of magnification will be limited by the fact that the picture must include a sufficient number of grain [21-23].

1.2 Estimation of Ferrite Grain Size

When ferrite nucleation occurs homogeneously in the austenite matrix, ferrite grain is independent of austenite grain size. In the case that ferrite nucleation occurs at austenite grain corners, ferrite grain size is proportional to d'_v . The ferrite grain size is determined by the number of ferrite nucleations at austenite grain surfaces until these surfaces are completely occupied by ferrite grains. During cooling, ferrite grains are nucleated and grown at each temperature with corresponding nucleation and growth rates. On the temperature T_i ferrite nucleates at the rate

$I_s(T_i)$ and grows at the rate $\alpha(T_i)$, where $I_s(T_i)$ and $\alpha(T_i)$ are the nucleation rate and the parabolic rate constant in the isothermal transformation at temperature T_i [24]. Ferrite grains number n_a nucleated at temperature T_a during cooling was calculated by Umemoto et al. [25] as

$$n_a = I_s(T_a) dt_a = \left[\frac{I_s(T_a)}{Q(T_a)} \right] dT \quad (4)$$

where $Q(T_a) = -dT/dt$ is the cooling rate. Assuming that, ferrite nucleation occurs at n_a is proportional to CR^n , where CR and n_1 are the cooling rate. If ferrite nucleation occurs at austenite grain edges & corners, n_a is proportional to CR^{n_2} and CR^{n_3} . Ferrite grain size can be calculated as follows [25, 26]

$$d_\alpha = \left(\frac{2}{3S_{gb}n_\alpha} \right)^{\frac{1}{3}} \quad (5)$$

where S_{gb} is the austenite grain surface area per unit volume.

As increasing the austenite grain size and decreasing the cooling rate, ferrite grain size is increased. Determining the prior austenite grain size in heat treatment of microalloyed steels, one may substitute by the austenitising time t and temperature T as below [7, 27]

$$d_y = k_1 t^{k_2} \exp\left(\frac{-Q}{RT}\right) \quad (6)$$

where positive constants are k_1 , k_2 , & Q . Therefore, the ferrite grain size is derived from Eq. (10) and (9) as follows

$$d_\alpha = a \exp\left(\frac{-A}{T}\right) (CR)^{-n} t^m \quad (7)$$

where positive constants are a , A , n , & m . Using this equation and measuring the austenitising time, temperature, and cooling rate, the ferrite grain size of the 22MnVNb6 Microalloyed Steel can be estimated. The estimated ferrite grain size and the Hall-Petch relationship from Eq. (1) determine the yield strength of this steel.

2 Experimental Procedure

With different austenitising times, temperatures, and cooling rates from the tests of heat treatment were carried out to determine of values a , A , n , & m from Eq. (7). A commercial strip of 22MnVNb6 microalloyed low carbon cast steel 30.00 mm long, with a rectangular cross section, 20.00 mm wide by 5.00 mm thick was applied on the tests [28-31]. The research material having chemical composition showed in Table 1. Surface processing operations for property enhancing to determine the d_α , the test of heat treatment programmes are showed in Table 2 and have been utilized. Using thermocouple to determine the cooling rate of each specimen, it was utilized to record the data of temperature at austenitising time 1 s. Transmission electron

Table 1 Chemical composition of a 22MnVNb6 Microalloyed Steel in As-Cast State used in this research work, wt-%

C	Mn	Si	P	S	Cu	Ni	V	Ti	Nb	Al	N
0.22	1.39	0.38	0.017	0.017	0.22	0.16	0.09	0.01	0.05	0.079	0.017

Table 2 The test of heat treatment programmes used in this research study (using Eq. (8) to determine the d_a)

Austenitising temperature, °C	Austenitising time, (s)	Cooling rate, °C/s	d_a (μm)
900	660	60,40,12,6.3,5	15.8,17.0,21.4,24.2,25.3
	840	60,40,12,6.3,5	17.2,18.6,23.4,26.4,27.6
	1020	60,40,12,6.3,5	18.5,20.0,25.1,28.4,29.7
	1230	60,40,12,6.3,5	19.8,21.4,26.9,30.4,31.8
1000	680	60,35,15,9,7	22.7,25.2,29.6,32.6,34.2
	860	60,35,15,9,7	24.8,27.4,32.2,35.5,37.3
	1040	60,35,15,9,7	26.6,29.4,34.6,38.1,40.0
	1220	60,35,15,9,7	28.2,31.2,36.7,40.4,42.4

Table 3 Size distribution of austenite grain of microalloyed steel in as-cast state

Steel	Range of chord lengths, μm	Number of chords per mm, $N_L(f)$	Diameter of grains, mm, d_j	Number of grains per mm^3 , $N_v(j)$	Evaluated mean grain size, μm , \bar{d}
22MnVNb6	0-170	231	0.017-0.170	1.5417×10^5	36.1

microscopy (TEM) was the most widely used technique for studying all aspects of phase transformations in steels over the length scale range 1–100 nm [32]. TEM data was used as a starting point for the proposed model in micromagnetic simulation for electrodeposited nickel nanowires [33]. Defects created by the superelastic cycling in thin Ni–Ti wires were analyzed by TEM [34]. TEM studies were carried out on the some samples of the as-cast state and the heat treatment test. Optical microscopy was used to examine the microstructure of the microalloyed steel specimen in as-cast state and the heat treatment test. In order to determine the microstructure, the samples are specially etched in 5% nital solution [9]. The concentration of the nital solution has to be adjusted for different samples. The microstructure is then measured at magnification 50x using a filler eyepiece. It was observed that the microstructures consisted of ferrite and a small amount of pearlite. The classic data in the literature for the grain size dependence of the strength in many metals are reviewed [13]. The ferrite microstructure determination should be done in a magnification suited to the size of the grain so that small grains may not be lost. The degree of magnification will be limited by the fact that the picture must include sufficient ferrite grain size. The ferrite grain size of each specimen was measured according to ISO 643 standard. To determine yield strength of the as-cast state steel of a 22MnVNb6 microalloyed, the different ferrite grain size microstructures of the steel were determined and calculated by using the Spektor equation and extended Hall-Petch relationship. After calculating a , A , n , and m in Eq. (7) and the extended Hall-Petch relationships for the low carbon microalloyed steel, some heat treatment as the annealing was carried out in order to compare estimated ferrite grain size and strength data.

3 Result and Discussion

The annealing was already used to improve the tensile and hardness properties of the 22MnVNb6 microalloyed low carbon cast steel in as-cast state. Since the austenite and ferrite grain size of microalloyed steel are important factor, they were necessary to show the grain size with austenite and ferrite as in Fig. 1 and ferrite-pearlite micrograph of heat treated as annealing in Fig. 2. The microstructures were examined using light microscopy and by transmission electron microscopy of thin foils. Representative TEM images of a 22MnVNb6 microalloyed steel are given on as-cast state in Fig. 3 and on the austenitising temperature at 1000 °C in Fig. 4 [35, 36]. The austenite grain size of the as-cast microalloyed steels were investigated using Spektor's analysis in order to determine the size distribution. The prior austenite grain boundaries were revealed by etching the specimens for evaluated the mean grain size. Table 3 shows size distribution of austenite grain and Table 4, there is comparison between the mean austenite grain size of Spektor's method and the values of G , \bar{d} & l of International standard [10, 37-40]. The microalloyed steel was studied investigated to optimize the influence of single and multiple microalloying additions on the ferrite grain size microstructure in as-cast state. Ferrite grain size distributions can be recorded by photographing the microscopic picture and the determination requires measurement of each individual grain. Ferrite grain size distribution in one dimension is the distribution of the lengths of linear intercepts through the grains. Metallographic techniques for measuring ferrite grain size were originally based on point counting or linear intersection length distribution. The ferrite grain size of microalloyed steel is important factors, on Table 5 shows size distribution and grain size contribution to yield stress. Table 6 shows estimation of

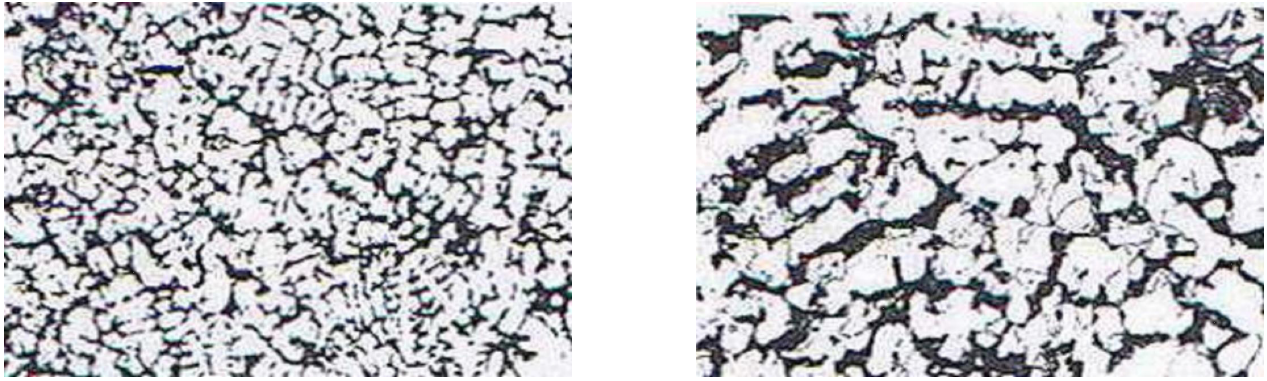



Fig. 1 On the left, austenite grain size microstructure of the steel 22MnVNb6 in as-cast state, as 100 μm , on the right, ferrite grain size microstructure of the same steel as 100 μm , using 2 magnifications according to show some importance of pearlite



Fig. 2 The 100 μm () ferrite-pearlite micrograph of heat treated as annealing samples of steel 22MnVNb6, 900°C (left), and 1000°C (right)

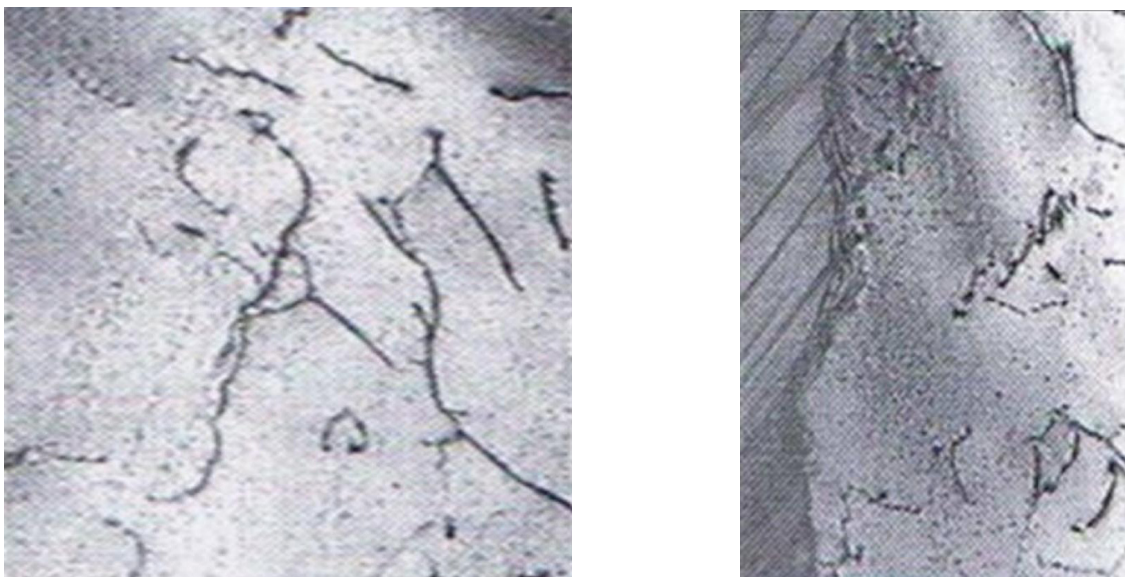



Fig. 3 On the TEM, foil, BF as 0.2 μm , the left as ferrite microstructure of steel 22MnVNb6 and the right as interface between ferrite and pearlite of the same steel

Table 4 Comparison of austenite mean grain size determined by Spektor's method with estimated austenite grain characteristics according to International standard (ISO643)

Steel	Evaluated mean grain size, μm , d	Estimated grain size (Index), G	Mean diameter of grain, μm , d	Mean intersected segment, μm , l
22MnVNb6	36.1	6.5	37.7	34.2

Table 5 Size distribution of ferrite grains and grain size contribution to yield stress of microalloyed steel in as-cast state

Steel	Range of chord lengths, μm	Number of chords per mm, $N_L(j)$	Diameter of grains, mm, d_j	Number of grains per mm^3 , $N_v(j)$	Evaluated mean grain size, $\mu\text{m}, d$	$Kd_\alpha^{-0.5}$ (MPa)
22MnVNb6	0-130	625	0.013 -0.130	14.0886×10^5	20.2	140.8

Table 6 Estimation of yield strength of microalloyed steel on the test of heat treatment programmes, based on extended Hall-Petch relationship, with comparative mechanical properties addition

Microalloyed Steel	Heat Temp. ($^\circ\text{C}$)	R_o	ΔR_α	ΔR_g	ΔR_p	ΔR_t	R_y (MPa)	Vickers Hardness (HV_{10})	Tensile Strength (σ_u ; MPa)
22MnVNb6	900	40	121	169	21	73	424	186	639
	1000	40	121	143	38	98	440	187	651

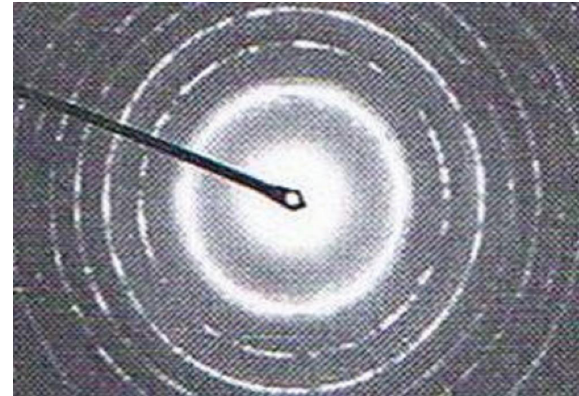


Fig. 4 (Left) According to the X 20 k precipitates of ferrite grain size of the steel 22MnVNb6, (right) using the diffraction pattern TEM replica, SAD, for austenitising temperature at the 1000 $^\circ\text{C}$ to find those precipitates of the steel

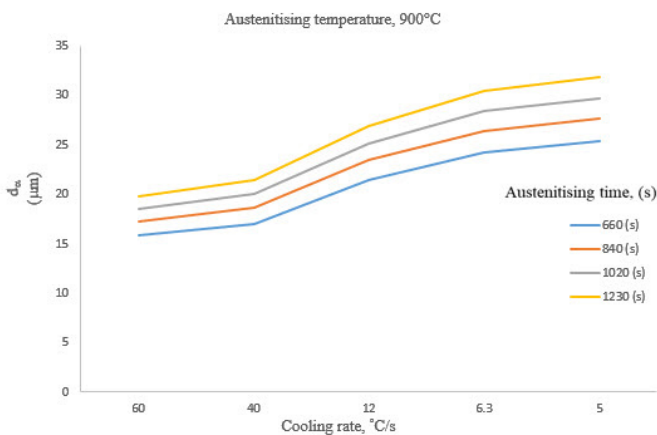


Fig. 5 Graph of ferrite grain size on cooling rate using austenitising temperature 900 $^\circ\text{C}$, as shown orange graph of austenitising time 1230 (s), blue graph of 1020 (s), red graph of 840 (s), and azure graph of 660 (s)

$$d_\alpha = 18152 \exp\left(\frac{-10174}{T}\right) (CR)^{-0.19} t^{0.37} \quad (8)$$

Where d_α , CR , t , and T are expressed in μm , $^\circ\text{C}/\text{s}$, s , and K , respectively.

Considering the experimental results showed in Fig. 4 and 5 and Eq. (8), by increasing the austenitising time and temperature and decreasing the cooling rate, the ferrite grain size transforming from austenite is increased. In fact, by increasing the austenitising time and temperature, the prior austenite grain size is increased, and nucleation sites for ferrite formation are decreased. Atom possessing an energy level of the reactants and activation energy will have sufficient energy to react spontaneously to reach the reacted state of energy of the products [41]. A basic procedure for determining the activation energy was developed by Conrad and Wiedersich [42]. By decreasing the cooling rate, the activation energy for nucleation is decreased and a smaller number of ferrite nucleation sites produce large ferrite grain size.

4 Conclusions

The Hall-Petch relationship can be utilized to examine the dependence of yield stress on ferrite grain size of the as-cast state steel, but extended Hall-Petch relationship can be utilized of the betterment that on the test of heat treatment programmes. When increased by the austenitising temperature, the effects

yield strength of microalloyed steel on the test of heat treatment programmes, based on extended Hall-Petch relationship, with comparative mechanical properties addition. To determine the α , A , n , and m values in Eq. (8) for the test microalloyed steel, graphs of d_α versus t for different austenitising temperature and cooling rates were plotted, as presented in Fig. 4 and 5. It is interesting to note that, as these figures show, the experimental relationships between d_α , t , and CR are linear. This is accordance with Eq. (8). Referring to graphs of d_α versus t the ferrite grain size can be expressed as

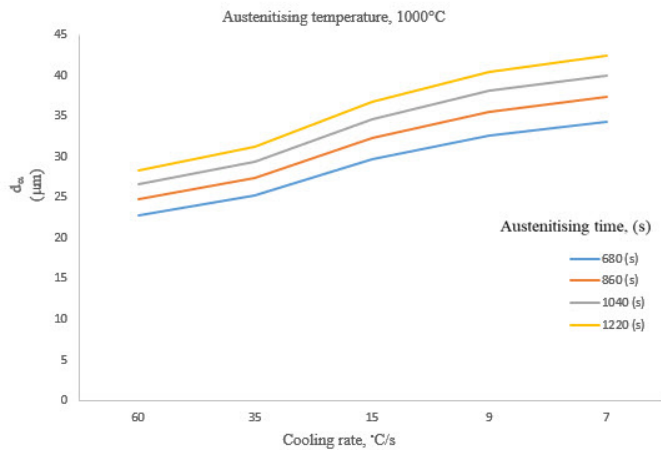


Fig. 6 Graph of ferrite grain size on cooling rate using austenitising temperature 1000°C, as shown orange graph of austenitising time 1220 (s), blue graph of 1040 (s), red graph of 860 (s), and azure graph of 680 (s)

of austenitising time and cooling rate on ferrite grain size are decreased. When d_{α} formed by continuous cooling transformation, is decreased with an increase in cooling rate or decrease in austenitising time and temperature, the d_{α} can be shown as in Eq. (8). Also, it's good correlation between experimental and estimated ferrite grain size, yield stress of the material studied of this research work.

Acknowledgements

The authors would like to express their gratitude to K. Macek, Faculty of Mechanical Engineering, Czech Technical University in Prague, Czech Republic, for his help with some experiments, discussions, the Strategic Wisdom and Research Institute, Srinakharinwirot University and the Srinakharinwirot University, Thailand. This research was funded by the Srinakharinwirot University budget in the fiscal year 2551, under the Project agreement 151/2551 is acknowledged and for the consent to publish this paper.

References

[1] Gladman, T. "The Physical Metallurgy of Microalloyed Steels." 1st Ed., The University Press, Cambridge, London, 1997.

[2] Gladman, T., McIvor, I. D., Pickering, F. B. "Some aspects of the structure-property relationships in high-carbon ferrite-pearlite steels." *Journal of the Iron and Steel Institute*. 210(12), pp. 916-930. 1972.

[3] Campbell, P. C., Hawbolt, E. B., Brimacombe, J. K. "Microstructural engineering applied to the controlled cooling of steel wire rod: Part II. Microstructural evolution and mechanical properties correlations." *Metallurgical Transactions A*. 22(11), pp. 2779-2790. 1991. <https://doi.org/10.1007/BF02851372>

[4] Porter, D. A., Easterling, K. E., Sherif, M. Y. "Phase Transformations in Metals and Alloys." 3rd Ed., CRC Press, Taylor & Francis Group, 2009.

[5] Umamoto, M., Guo, Z. H., Tamura, I. "Effect of cooling rate on grain size of ferrite in a carbon steel." *Materials Science and Technology*. 3(4), pp. 249-255. 1987. <https://doi.org/10.1179/mst.1987.3.4.249>

[6] Brooks, C. R. "Principles of the Austenitization of Steels." Elsevier Science Publishers LTD, U.K., 1992.

[7] Pluphrach, G. "Effect of vanadium additions on yield stress of low carbon microalloyed cast steels." *Srinakharinwirot Science Journal*. 19-21, pp. 102-108. 2003-2005.

[8] Pluphrach, G. "Study of the effect of solidification on graphite flakes microstructure and mechanical properties of an ASTM a-48 gray cast iron using steel molds." *Songklanakar Journal of Science and Technology*. 32(6), pp. 613-618. 2010.

[9] Macek, K., Cejj, J., Pluphrach, G. "Yield strength of low carbon cast steels." In: Workshop, Department of Materials Engineering, Faculty of Mechanical Engineering, CTU, Prague, Czech Republic, pp. 446-447. 2005.

[10] International Standard (ISO643). "Steels-Micrographic Determination of the Apparent Grain Size." 2nd Ed. 2003.

[11] DeHoff, R. T., Rhines, F. N. "Quantitative Microscopy." McGraw-Hill Book Company, New York, pp. 10-15. 1968.

[12] Elwazri, A. M., Essadigi, E., Yue, S. "The kinetics of static recrystallization in microalloyed hypereutectoid steels." *ISIJ International*. 44(1), pp. 162-170. 2004. <https://doi.org/10.2355/isijinternational.44.162>

[13] Dunstan, D. J., Bushby, A. J. "Grain size dependence of the strength of metals: The Hall-Petch effect does not scale as the inverse square root of grain size." *International Journal of Plasticity*. 53, pp. 56-65. 2014. <https://doi.org/10.1016/j.ijplas.2013.07.004>

[14] Counts, W. A., Braginsky, M. V., Battaile, C. C., Holm, E. A. "Predicting the Hall-Petch effect in fcc metals using non-local crystal plasticity." *International Journal of Plasticity*. 24(7), pp. 1243-1263. 2008. <https://doi.org/10.1016/j.ijplas.2007.09.008>

[15] Wang, W., Yan, W., Zhu, L., Hua, P., Shan, Y., Yang, K. "Relation among rolling parameters, microstructures and mechanical properties in an acicular ferrite pipeline steel." *Materials and Design*. 30(9), pp. 3436-3443. 2009. <https://doi.org/10.1016/j.matdes.2009.03.026>

[16] Martis, C. J., Putatunda, S. K., Boileau, J. "Processing of a new high strength high toughness steel with duplex microstructure (Ferrite+Austenite)." *Materials and Design*. 46, pp. 168-174. 2013. <https://doi.org/10.1016/j.matdes.2012.10.017>

[17] Azghandi, S. H. M., Ahmadabadi, V. G., Raoofian, I., Fazeli, F., Zare, M., Zabet, A., Reihani, H. "Investigation on decomposition behavior of austenite under continuous cooling in vanadium microalloyed steel (30MSV6)." *Materials and Design*. 88(25), pp. 751-758. 2015. <https://doi.org/10.1016/j.matdes.2015.09.046>

[18] Wei, H., Liu, G. "Effect of Nb and C on the hot flow behavior of Nb microalloyed steels." *Materials and Design*. 56, pp. 437-444. 2014. <https://doi.org/10.1016/j.matdes.2013.11.009>

[19] Wei, H., Liu, G., Zhao, H., Kang, R. "Hot deformation behavior of two C-Mn-Si based and C-Mn-Al based microalloyed high-strength steels: A comparative study." *Materials and Design*. 50, pp. 484-490. 2013. <https://doi.org/10.1016/j.matdes.2013.03.043>

[20] Li, X., Duan, L., Li, J., Wu, X. "Experimental study and numerical simulation of dynamic recrystallization behavior of a micro-alloyed plastic mold steel." *Materials and Design*. 66(Part A), pp. 309-320. 2015. <https://doi.org/10.1016/j.matdes.2014.10.076>

[21] Pereloma, E. V., Kostryzhev, A. G., AlShahrani, A., Zhu, C., Cairney, J. M., Killmore, C. R., Ringer, S. P. "Effect of austenite deformation temperature on Nb clustering and precipitation in microalloyed steel." *Scripta Materialia*. 75(15), pp. 74-77. 2014. <https://doi.org/10.1016/j.scriptamat.2013.11.026>

[22] Zou, T., Li, D., Wu, G., Peng, Y. "Yield strength development from high strength steel plate to UOE pipe." *Materials and Design*. 89(5), pp. 1107-1122. 2016. <https://doi.org/10.1016/j.matdes.2015.10.095>

- [23] Zhu, Y. Z., Wang, S. Z., Li, B. L., Yin, Z. M., Wan, Q., Liu, P. "Grain growth and microstructure evolution based mechanical property predicted by a modified Hall–Petch equation in hot worked Ni76Cr19AlTiCo alloy." *Materials and Design*. 55, pp. 456–462. 2014.
<https://doi.org/10.1016/j.matdes.2013.10.023>
- [24] Dahlberg, C. F. O., Faleskog, J. "Strain gradient plasticity analysis of the influence of grain size and distribution on the yield strength in polycrystals." *European Journal of Mechanics A/Solids*. 44, pp. 1–16. 2014.
<https://doi.org/10.1016/j.euromechsol.2013.09.004>
- [25] Umemoto, M., Ohtsuka, H., Tamura, I. "Grain size estimation from transformation kinetics." *Acta Metallurgica*. 34, pp. 1377–1385. 1986.
[https://doi.org/10.1016/0001-6160\(86\)90025-8](https://doi.org/10.1016/0001-6160(86)90025-8)
- [26] Umemoto, M., Guo, Z. H., Tamura, I. "Effect of cooling rate on grain size of ferrite in a carbon steel." *Materials Science and Technology*. 3, pp. 249–255. 1987.
<https://doi.org/10.1179/mst.1987.3.4.249>
- [27] Brooks, C. R. "Principles of the Austenitization of Steels." Elsevier Science Publishers LTD, U.K., 1992.
- [28] Barai, P., Weng, G. J. "Mechanics of a nanocrystalline coating and grain-size dependence of its plastic strength." *Mechanics of Materials*. 43(9), pp. 496–504. 2011.
<https://doi.org/10.1016/j.mechmat.2011.06.006>
- [29] Lim, H., Lee, M. G., Kim, J. H., Adams, B. L., Wagoner, R. H. "Simulation of polycrystal deformation with grain and grain boundary effects." *International Journal of Plasticity*. 27, pp. 1328–1354. 2011.
<https://doi.org/10.1016/j.ijplas.2011.03.001>
- [30] Hug, E., Dubos, P. A., Keller, C., Duchêne, L., Habraken, A. M. "Size effects and temperature dependence on strain-hardening mechanisms in some face centered cubic materials." *Mechanics of Materials*. 91(1), pp. 136–151. 2015.
<https://doi.org/10.1016/j.mechmat.2015.07.001>
- [31] Lavergne, F., Brenner, R., Sab, K. "Effects of grain size distribution and stress heterogeneity on yield stress of polycrystals: A numerical approach." *Computational Materials Science*. 77, pp. 387–398. 2013.
<https://doi.org/10.1016/j.commatsci.2013.04.061>
- [32] Boyd, D., Yao, Z. "Application of modern transmission electron microscopy (TEM) techniques to the study of phase transformations in steels." *Phase Transformations in Steels*. Vol. 2 (pp. 507–531.) 2012.
<https://doi.org/10.1533/9780857096111.4.507>
- [33] França, C. A., Guerra, Y., Valadão, D. R. B., Holanda, J., Padrón-Hernández, E. "Transmission electron microscopy as a realistic data source for the micromagnetic simulation of polycrystalline nickel nanowires." *Computational Materials Science*. 128(15), pp. 42–44. 2017.
<https://doi.org/10.1016/j.commatsci.2016.11.007>
- [34] Delville, R., Malard, B., Pilch, J., Sittner, P., Schryvers, D. "Transmission electron microscopy investigation of dislocation slip during superelastic cycling of Ni–Ti wires." *International Journal of Plasticity*. 27(2), pp. 282–297. 2011.
<https://doi.org/10.1016/j.ijplas.2010.05.005>
- [35] Lefebvre, S., Devincere, B., Hoc, T. "Yield stress strengthening in ultrafine-grained metals: A two-dimensional simulation of dislocation dynamics." *Journal of the Mechanics and Physics of Solids*. 55(4), pp. 788–802. 2007.
<https://doi.org/10.1016/j.jmps.2006.10.002>
- [36] Najafi, H., Rassizadehghani, J., Norouzi, S. "Mechanical properties of as-cast microalloyed steels produced via investment casting." *Materials and Design*. 32(2), pp. 656–663. 2011.
<https://doi.org/10.1016/j.matdes.2010.08.007>
- [37] Głownia, J., Kalandyk, B. "Effect of precipitation strengthening in low alloyed Mn–Ni cast steels." *Journal of Materials Processing Technology*. 207(1–3), pp. 147–153. 2008.
<https://doi.org/10.1016/j.jmatprotec.2007.12.097>
- [38] Zhao, J., Jiang, Z., Lee, C. S. "Enhancing impact fracture toughness and tensile properties of a microalloyed cast steel by hot forging and post-forging heat treatment processes." *Materials and Design*. 47, pp. 227–233. 2013.
<https://doi.org/10.1016/j.matdes.2012.11.051>
- [39] Korczak, P. "Influence of controlled rolling condition on microstructure and mechanical properties of low carbon micro-alloyed steels." *Journal of Materials Processing Technology*. 157–158(20), pp. 553–556. 2004.
<https://doi.org/10.1016/j.jmatprotec.2004.07.113>
- [40] Kazeminezhad, M., Taheri, A. K. "Prediction of ferrite grain size and tensile properties of a low carbon steel." *Materials Science and Technology*. 20(1), pp. 106–110. 2004.
<https://doi.org/10.1179/174328413X13789824293704>
- [41] Smith, W. F. "Principles of Materials Science and Engineering." 2nd Ed., McGraw-Hill International Editions, Singapore, 1990.
- [42] Reed-Hill, R. E. "Physical Metallurgy Principles." 3rd Ed., PWS Publishing Company, Boston, M.A., U.S.A., 1994.